Investigating Structural Changes in the Surface Morphology of Proton-Irradiated Polydimethylsiloxane

Tyler Billings, Tanner Kirkpatrick, Madison LaCroce, Paul McDonnell,
Dylan Mosquera, Justin Myers, Elliot Snider, Sam Wilensky

December 17, 2016

Abstract

The widespread use of silicone in the construction of satellites necessitates an improved understanding of the interaction between charged particles and the material under the conditions of space. Previous research into the optical degradation of polydimethylsiloxane (PDMS) under low energy ($<$200keV) proton irradiation has produced trends in surface morphology, such as cracking and discoloration, dependent on the fluence applied to the sample. Samples of PDMS were subjected to two novel surface treatments: oxidation and slide separation. Preliminary results have exhibited new morphological effects not previously seen in the literature.

Introduction

A Single Event Effect is an event in which a single energized particle strikes and damages sensitive pieces of electronic equipment. These effects range anywhere from damage of circuitry and memory cells to creating high operating currents. An example of a Single Event Effect is Qantas Flight 72. In 2008, this flight experienced an electrical malfunction that sent the flight into a sudden downward pitch. After investigation, it was determined that the malfunction was caused by a single energized (MeV) particle that resulted from a cosmic ray. These cosmic rays penetrated the lower atmosphere, producing charged particles that interrupted electrical communications on board Qantas Flight 72 [Booz]. Events like this force aircraft and satellite designers to consider how components of the craft behave in the presence of these cosmic rays [LaBel].

However, not all types of cosmic rays are considered when designing these crafts. For example, in 1999, NASA launched its Chandra telescope into orbit. The Chandra was built so that its sensors and systems would be protected from the high energy (MeV) irradiation it would encounter in orbit. After a short period of time, NASA began to receive images from the Chandra. However, the image quality was much worse than expected. The only explanation for this loss of quality was that the silicone used to seal and bind the imaging electronics was damaged, exposing the delicate electrical systems to radiation. Because NASA had prepared the Chandra for high energy (MeV) particle radiation, it was concluded that the damage was caused by low energy (keV) particles [Weisskopf][Prigozhin]. This event motivated scientists to study how silicone rubbers behave under low energy particle irradiation.

Much research into the effects of low energy particle irradiation on degradation of silicone has focused on proton irradiation of polydimethylsiloxane (PDMS), a versatile polymer that is utilized in a wide range of disciplines and functions. The chemical and physical properties of PDMS make it a desirable sealant, binder, and mold for applications in the aerospace industry [Gonzlez-Prez]. Xiao *et al.* studied optical degradation of PDMS irradiated with low energy protons (150keV) [Xiao *et al.*]. Similar studies done by Zhang *et al.* and Di *et al.* examined the optical degradation of methyl silicone rubbers under low energy proton irradiation. Zhang *et al.* irradiated methyl silicone rubber with 200 keV protons, while Di *et al.* irradiated methyl silicone rubber using 150 keV protons [Zhang *et al.*][Di *et al.*]. In Di's experiments, the silicone samples were reinforced with TiO_2 nanoparticles or MQ silicone resin with the goal of improving its resistance

to degradation under proton irradiation [Di *et al.*]. The overarching goals of these experiments were to understand how PDMS behaves under low energy proton irradiation and how different preparation and treatments of the silicone samples affect their resistance to proton irradiation.

The work to date at Gettysburg College has aimed to replicate the results of previously published literature. During the summer of 2016, Alex Grun irradiated samples of PDMS using low energy protons ($90 - 150$ keV). Grun implemented a novel surface treatment as well as new methods for PDMS sample preparation in order to further understand how PDMS responds to proton irradiation. Grun oxidized the surface of PDMS to see if its resistance to proton irradiation changed. Additionally, he prepared PDMS samples both directly on glass slides and separately in a petri dish [Grun]. Previous experiments' failure to specify the nature of their sample preparation prompted the investigation of this preparation method. Motivated by Grun's results, we investigated the structural changes of the surface morphology of proton irradiated PDMS samples. The goals of our experiment are to both replicate results from published literature and to expand on Alex Grun's research. After irradiating samples, we will examine the effects of oxidation and sample preparation on the proton irradiated PDMS. We will also use computer software to quantify the surface damage on our irradiated samples of PDMS.

Experimental

PDMS is a form of organic silicone made up of chains of Si-O bonds. These bonds are particularly strong because of the π-bonds between the outer orbitals of the Si and O atoms. A π-bond occurs when the outer electrons of one atom overlap with the outer orbital of another and occupy the empty orbital of that atom. The result of the π–bond is a stable, strongly structured polymer. Figure 1 below shows the chemical structure of PDMS [AlbrightTech].

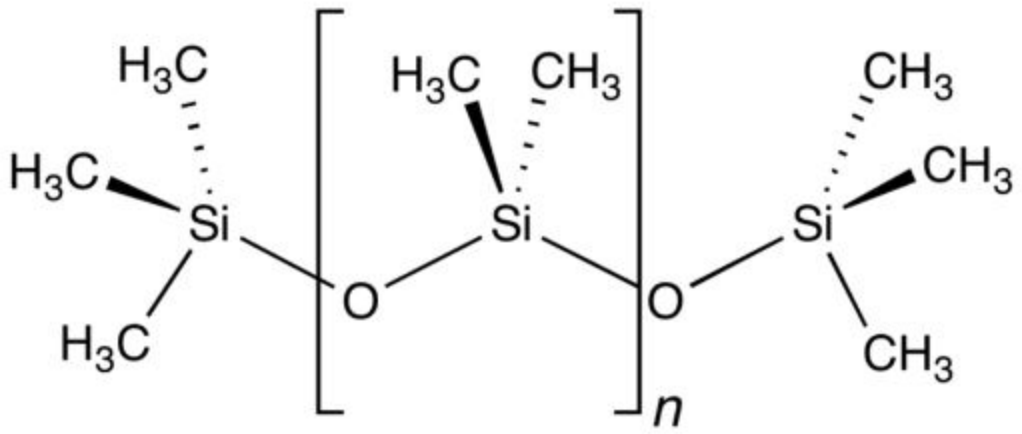

Figure 1: The chemical structure of PDMS. The dashed lines are bonds that go into the page (away from the viewer), the wedge bonds represent bonds that come out of the page (towards the viewer), and the straight lines are bonds that lie within the plane of the paper. The CH_3 groups around the siloxane backbone are known as methyl groups. The part of the compound surrounded by the brackets refers to the portion that is repeated based on the size of the PDMS, creating long strands of PDMS. [AlbrightTech]

Because of its structure, PDMS possesses many qualities that make it an optimal polymer for its application in spacecraft design. PDMS is an excellent electric insulator, exhibits hydrophobic behavior, is resistive to a wide range of temperatures, and is highly resistive to aging, ozone, and irradiation [Gonzlez-Prez]. In the aerospace field, PDMS and other methyl silicone rubbers are used as binding agents for solar cells because of their resistance to aging and irradiation, as well as their operative temperature range [Borjanovic *et al.* 2009].

Preparation of PDMS

The making of silicone is a three stage process. The first stage to making silicone involves producing chlorosilanes. In order to create chlorosilanes, pure silicon metal is mixed with chloromethane (CH_3Cl). This reaction creates three different types of chlorosilanes, with either one, two, or three organic compounds branching off the silicon. The most prevalent of these chlorosilanes is the type with two organic compounds and two chlorines. Once the chlorosilanes are produced, they undergo a reaction called hydrolysis. Hydrolysis is the process in which chemicals break down due to the addition of water. In this case, the chlorine breaks off of the chlorosilanes and is replaced with hydroxide (OH), creating a product called disilanol. The final stage of creating silicone is condensation polymerization, which introduces an acidic catalyst to remove the

hydrogen from the hydroxide in the disilanol. Once the hydrogen is removed, chains of silicon and oxygen begin forming, creating the silicone chains seen in Figure 2 [Industry].

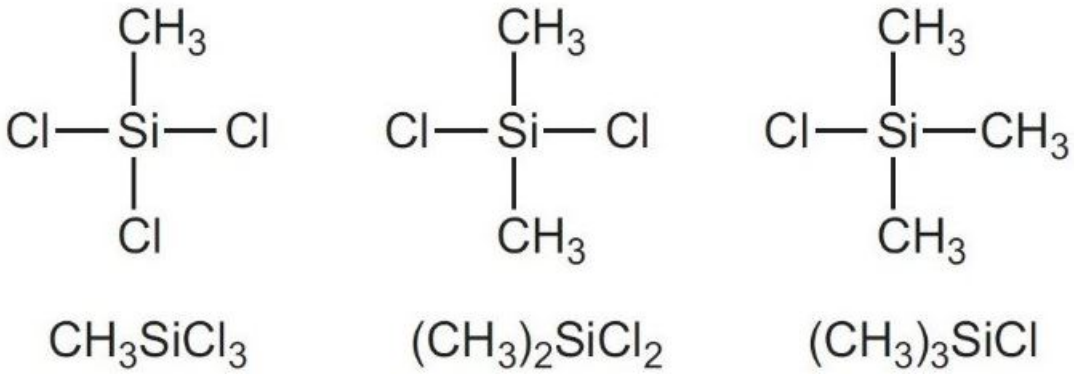

Figure 2: The three different types of chlorosilanes produced. The center formation (dimethyldichlorosilane) is most commonly produced because it is the most symmetric. This symmetry facilitates a faster chain production [Industry]. Entire reaction in Appendix.

In this experiment, we will use the Sylgard 184 elastomer kit to create our samples of PDMS. The Sylgard Kit utilizes two components: a base and a curing agent. The base is made up of silanes, which is the result of the first stage of silicone production, as mentioned above. The base is not necessarily made up of chlorosilanes, but this does not matter so long as the element replacing chlorine comes off in the hydrolysis step. The curing agent undergoes the second and third stage of silicone production simultaneously. By both adding water and an acidic catalyst, the curing agent initializes both hydrolysis and polymerization. We used a 10:1 ratio of base to curing agent for our PDMS samples.

PDMS is typically prepared by thoroughly mixing the base and curing components, then placing the liquid PDMS directly onto glass slides. After it is spread evenly over the slide, it cures in open air at STP. There are three methods we will use to dry the samples to change the behavior of PDMS during irradiation. The sample can be left out to dry in the open air, put into a vacuum, or placed in an oxidizer. PDMS that dries in a vacuum removes any air pockets left within and makes the samples' surface smoother [Allen]. Our samples had a thickness of 0.36 +/– 0.08 mm and were placed on long rectangular glass slides of thickness 1.11 +/– 0.01 mm. We will also be examining these samples using two novel treatment techniques, separation and oxidation. The following sections will discuss other methods of preparation and their related theories.

Sample Treatment: Separation

We have two methods of preparing our slides: separated and non–separated. Separated samples are prepared in a petri dish and then attached to our glass slides after the PDMS has dried. Non–separated samples refer to samples applied directly to the glass slide. These samples dry on the slides, and bind to the glass. By separating the samples from the slides, the overall surface tension of the PDMS decreases. This treatment should also change the charge distribution from the ionizing radiation in the chamber. The glass is an insulator and the air gap created behind the PDMS through separation, even with a microtour vacuum, is a less efficient insulation by about two orders of magnitude [Stephenson].

Sample Treatment: Oxidation

We will oxidize the surface of our samples to determine if this process effects PDMS's reaction to proton irradiation. In order to oxidize our PDMS, we place dry samples into the Bioforce Nanosciences UV/Ozone Pro Cleaner. This device uses a UV light source to produce ozone within the box, changing its internal atmosphere [Vig]. Additionally, a mercury sample within the box emits ozone, and when excited by a very specific wavelength of light, releases UV rays. Individually, the two agents are capable of oxidizing materials, but when used complimentarily, the process of oxidation has been found to be faster [Olah]. When PDMS undergoes oxidation, the chemical makeup of the surface changes. The ozone created by the UV light reacts with the surface silicone chains, adding a surface layer of silicone oxide. The longer the sample is subjected to oxidation, the more silicone oxide components are formed [Ouyang][Berdichevsky]. We oxidized our samples for one or six hours to see how these effects compared to unoxidized samples of PDMS.

CrossLinking

Cross–linking is the inter–connecting of polymer chains. Polymer chains of PDMS can be classified as either linear, branched, or cross–linked as shown in Figure 4.

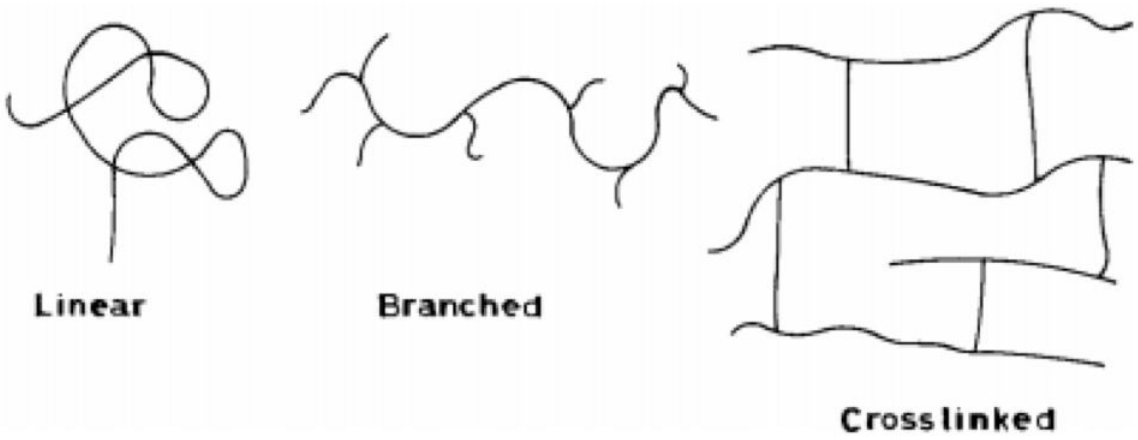

Figure 3: The three types of inter–connecting polymer chains. [Ebewele]

The branched chains of PDMS undergo cross–linking with one another when exposed siloxane groups bond with methyl groups from other chains. Cross–linking may also occur between methyl groups of two different polymer chains. Although scission and cross–linking occur naturally in the formation of the elastomeric state of the PDMS sample, we are most concerned with the extent of which these processes occur on the surface due to proton irradiation [Ebewele]. Cross–linking can occur as a result of random vibrations within the material. The energy of the vibrations is not essential in the process; the chain segments simply need to bump into each other.

Scission

The process of scission, in the case of proton irradiated PDMS, describes how polymer chains of PDMS are broken up. Scission occurs when energy from any source is added to the polymer chain. The elasticity of each polymer chain increases with its size, or n (Fig 1) value. As scission breaks down the polymer chains, the rigidity and brittleness of the PDMS increases. When the protons are irradiated onto the surface of the PDMS, longer chains break into shorter chains due to the energy of the protons incident on the PDMS surface. This is because the incident protons breaks the bond between the oxygen and silicon in the PDMS, separating them into smaller chains.

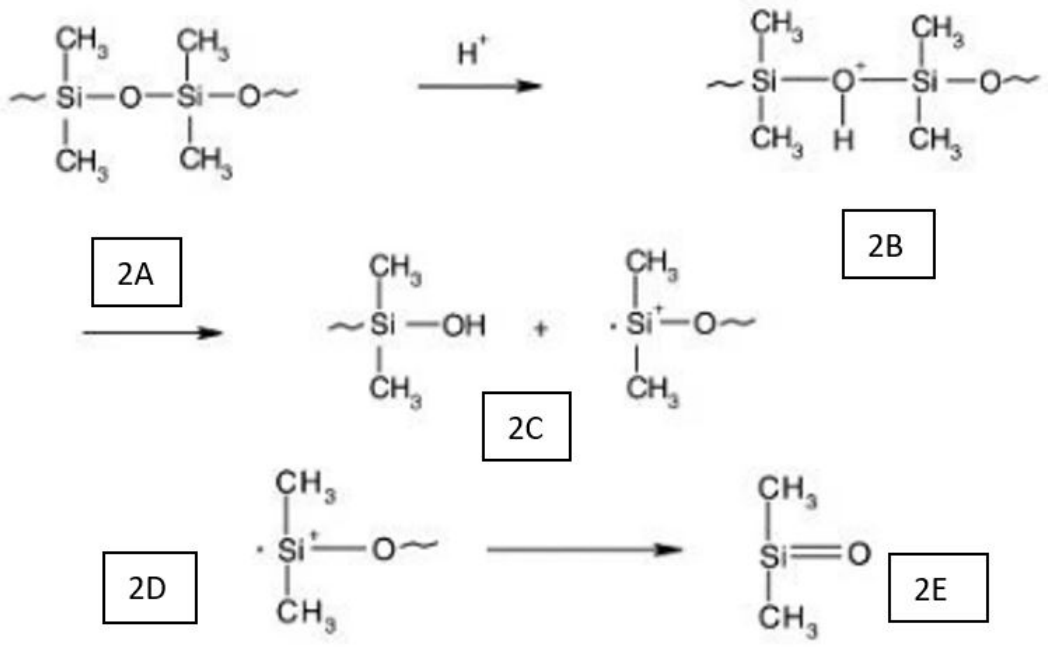

Figure 4: Diagram showing scission in PDMS due to the irradiation of protons. The protons (H+) bond with the oxygen atoms in the chain [2B] and weaken the Si-O bond due to the added positive charge, and the energy from the photon breaks this bond [2C]. The extra valence electron on the silicone is then used to form a double bond with the opposite side oxygen [2E][Zhang]

Experimental Setup

For this research, we used the Van de Graaff Positive Ion Accelerator (High Voltage Engineering Corp. Model PN–250) located at Gettysburg College to produce a beam of protons. The method we use in this experiment is identical to that of Booz *et al.* [Booz].

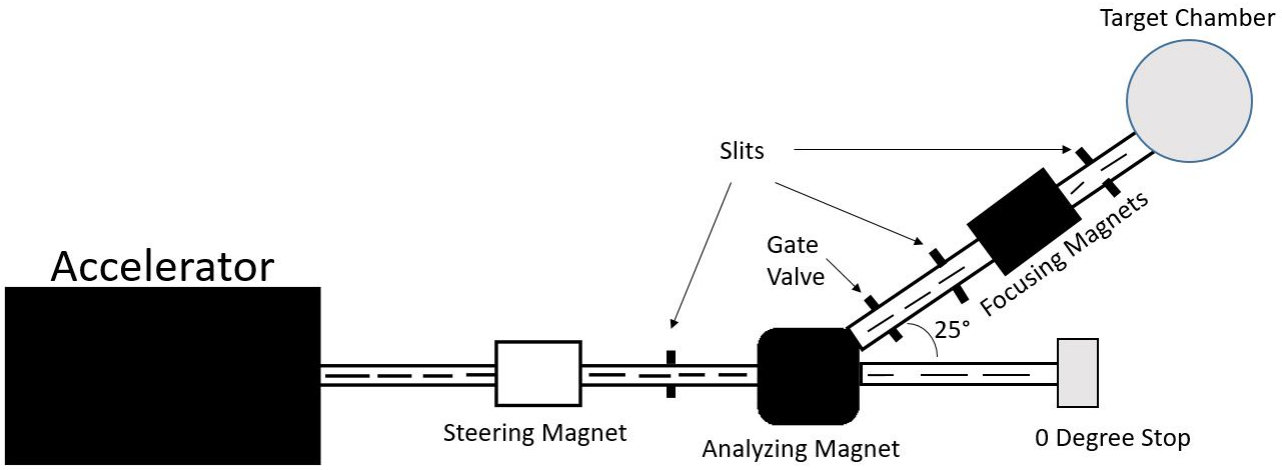

Figure 5: from murray, but Elliot remade it

Calculating Energy

When conducting each sample run, we need to know the energy level of the protons. Using previous work conducted by Murray, we created a graph of the energy of the protons versus the setting of the bending magnet. Murray found a relationship between the magnet settings and the energy of the protons. His entire data can be found in Appendix. We decided to modify his graph by only looking at the range of magnet settings that we used during our experiment. With the restricted, we applied a linear fit to the data shown in the Figure 6 below.

Using the equation of the linear fit, we were then able to relate the recorded magnet settings with the energy of the protons for each sample.

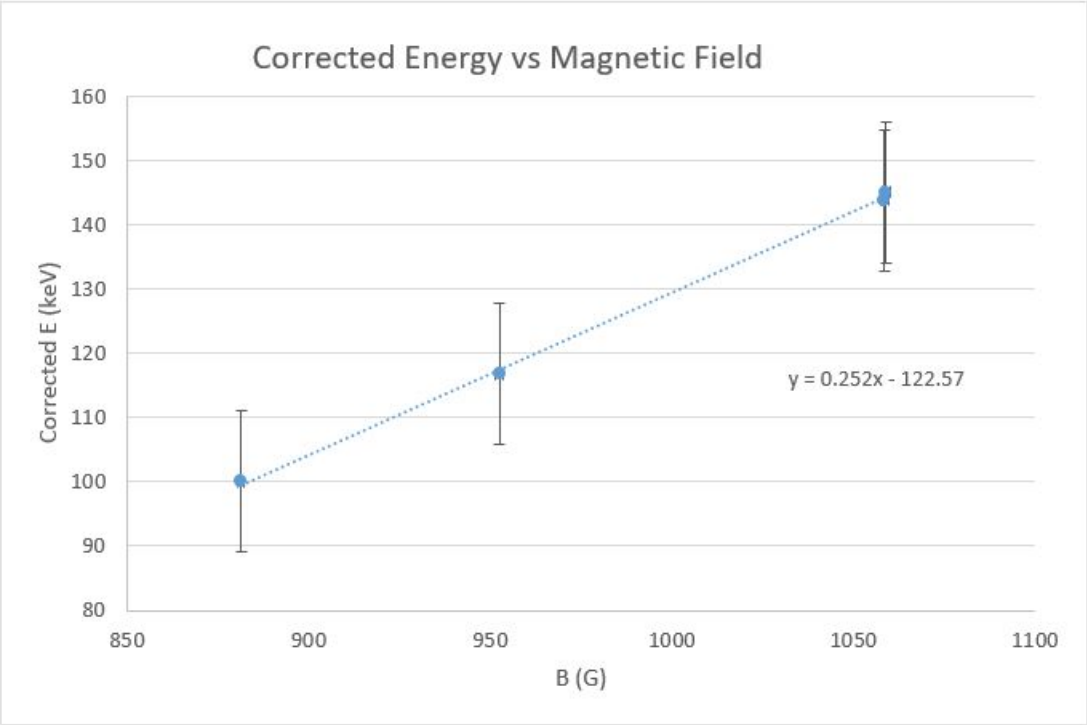

Figure 6: Linear fit of the relevant corrected energy and magnet settings from Murray's thesis

Target Chamber

The target chamber is an evacuated cylinder with a diameter of approximately 0.5 m, located at the end of the accelerator. The chamber contains a fixed target holder and two rotating arms, which are controlled outside of the target chamber. Three PDMS samples can be irradiated during each run without the need to open the chamber. The target chamber also contains electrical ports for detectors placed within the chamber to connect to external devices. At the entrance of the chamber, there is a small grid that is used to calculate fluence.

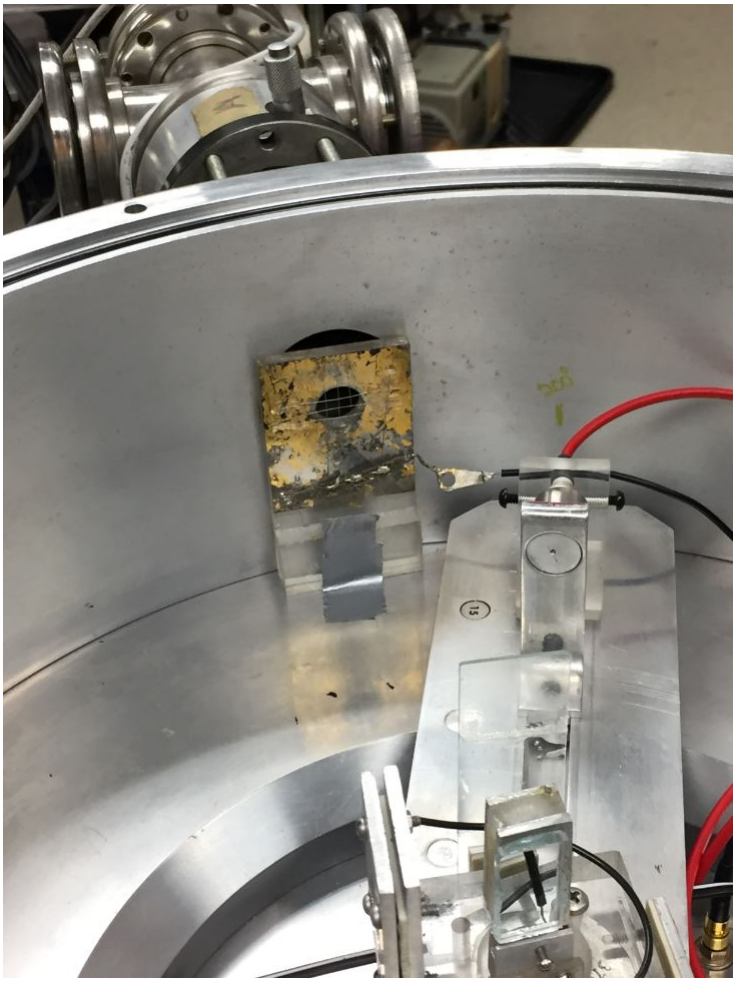

Figure 7: Interior photograph of the target chamber. A grid can be seen covering the entrance to the chamber. The three slide holders are pictured in the bottom right corner.

Fluence of the Proton Beam

Fluence describes the motion of particles through a given area. In our experiment, calculating the fluence of the proton beam is imperative to control the fluence levels. In order to calculate the fluence, we must make use of two measurements in the target chamber: the current measured at the metal grid, seen in Figure 7, and the current measured at the target location. Wires connected to the grid record each proton contacting the grid as an electronic pulse. These wires are connected to an Ortec 439 Digital Current Integrator, which measures the direct current of the grid. The charge of a proton is only 1.9×10^{-16} C, so the signal from the wires must be boosted by the 439. This device also assigns a Coulomb per pulse value, which designates a minimum input signal needed to generate an output signal. The continuous current is displayed on the front display panel (Ortec

439 Digital Current Integrator manual). The problem with this device is it that gives a continuous current. To obtain a discrete current, we connect the 439 to an Ortec 871 Timer and Counter, which reports the continuous current as a discrete current in numerical values (Ortec 871 manual). To measure the current of the target, wires are connected to a piece of metal at the target location. These wires connect to an oscilloscope, where we can read the current using the settings on the scope. The equation for fluence of a charged particle is as follows,

$$N_{particle} = I_T \Delta T \tag{1}$$

Here, $N_{particle}$ is the number of particles, I_T is the current measured at the target object or area, and ΔT is the time interval. This formula assumes a non-insulatory target. Since PDMS is an insulator, the current cannot be directly measured while the target is being irradiated. Instead, we use the current of the grid, which can be measured when the PDMS samples are irradiated. Equation (1) then becomes

$$N_{protons} = \frac{I_Y}{I_G} I_G \Delta T \tag{2}$$

where I_G is the current measured at the grid. The ratio of the measured target current before the PDMS is introduced and the grid current serves as a normalizing factor. During sample irradiation, the current of the grid and target are measured over identical 10 second time intervals in an independent measurement. Our final equation for calculating fluence is then

$$N_{protons} = (6.25 \times 10^{15}) \frac{I_T}{I_G} I_G \Delta T \tag{3}$$

Here, 6.25×10^{15} is a conversion factor determined by our settings on the Ortec 439. With this equation, currents at the grid and target tell us the desired time period required to irradiate PDMS samples to achieve a desired fluence. Due to the conversion factor, ΔT is no longer has units of time. Instead, we are given a number of counts correlating to the desired fluence displayed on the 871.

Results

Our first goal was to verify the previously published results of Xiao *et al.*, Zhang *et al.*,

and Di*et al.*. In Xiao *et al*s experiment, PDMS was irradiated by 150 keV protons at fluence levels ranging from 5×10^{14} cm^{-2} to 1×10^{16} cm^{-2}. They found that optical degradation occurred in the form of cracks at a fluence of 5×10^{14} cm^{-2} and higher. Zhang *et al.* irradiated samples of methyl silicone rubber with 200 keV protons. Zhang *et al.* found that the proton irradiation caused cracking on the surface of the methyl silicone rubber past a threshold fluence of 10^{15} cm^{-2}

We found that cracking on the surface of our samples began to occur at a fluence of about 8×10^{14} cm^{-2}. This value falls in between the threshold fluence found by Xiao *et al.* and Zhang *et al.*.

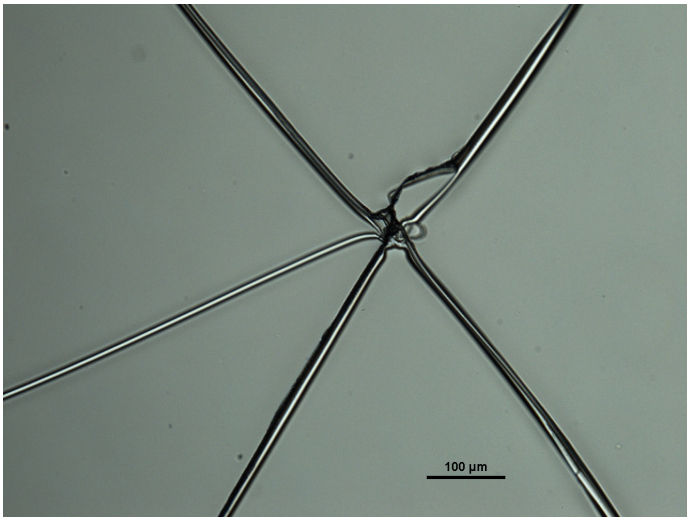

Figure 8: Cracking exhibited on a sample subjected to 1×10^{15} cm^{-2} fluence

During his research in the summer of 2016, Alex Grun discovered two different types of surface morphology on irradiated PDMS that had not been previously seen in published literature. One type exhibited patterns that looked like electric discharge, much like a lightning strike. The other pattern looked like a collection of organized, wave-like patterns. After irradiating samples ourselves, we found similar patterns appearing. With further investigation, we determined that these electric discharge patterns are known as Lichtenberg figures.

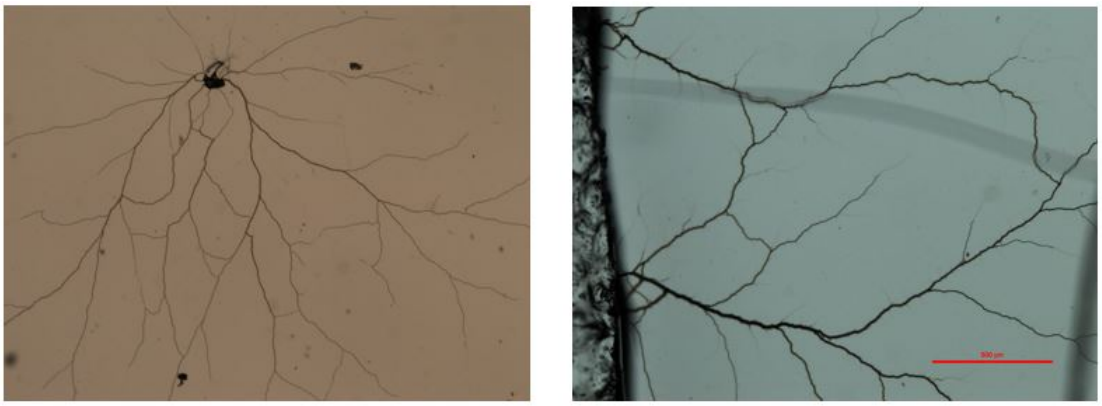

Figure 9: Images of electric discharge pattern. The left image shows an irradiated sample with fluence level of 1×10^{15} cm^{-2}. The right image was irradiated at a fluence of 1×10^{15} cm^{-2}.

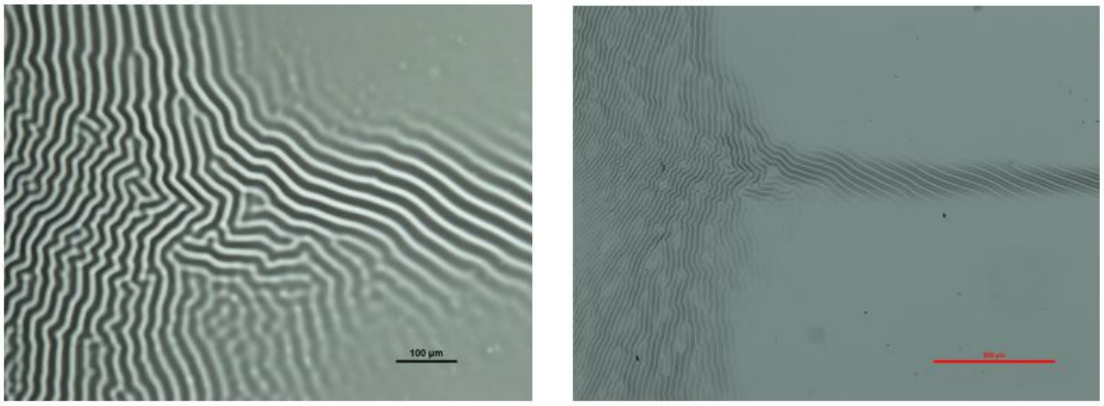

Figure 10: Images of ordered surface patterns. This sample was irradiated with 1×10^{15} cm^{-2}. Left image shows an irradiated sample at 4 times zoom. The Right image shows the same sample at 2 times zoom.

Discussion and Analysis

Cracking

The cracking we see on our samples of PDMS can be explained by the relationship between cross–linking and scission. As previously described, scission occurs when energy is added to the polymer chains. As the PDMS is irradiated, energy deposited on the surface causes scission, breaking bonds and increasing the number of branched polymer chains. These branched chains cross–link more easily than linear chains present before scission. As the energy incident on the sample increases, so does the prevalence of each process. Because only scission is energy dependent, it becomes the dominant process of the two when enough total energy is added to the system.

So as the fluence increases, more energy is added to the PDMS, causing scission to take over and cracks to be seen on the surface. We determined this threshold fluence to be around 8×10^{14} cm^{-2}. This threshold fluence falls between those determined by Xiao *et al.* and Zhang *et al.*. One reason for this disagreement is the flux of our proton beam. The flux of the proton beam describes the rate of fluence. It is possible that the time it takes to reach a desired fluence level influences the rates at which cross–linking and scission occur, thus determining the threshold fluence needed for cracking to occur.

Scission can occur in any polymer chain, regardless of the structure of the chain, as described by fluence. Zhang *et al.* affirmed that irradiating PDMS with low energy protons leads to more cross–linking within the PDMS, as seen by an elevated cross–linking density measured after proton irradiation. They found that with a fluence of less than 10^{15} cm^{-2}, cross–linking dominated. When they used a fluence greater than 10^{15} cm^{-2}, they found that surface degradation caused by scission dominated the sample, while cross–linking was less predominant [Zhang *et al.*]. This threshold was found by Xiao *et. al.* to be around a fluence of 5×10^{14} cm^{-2} [Xiao *et. al.*]. Cross–linking configurations are stronger than that of scission. Thus, as scission is the more dominant process occurring in PDMS, the surface is weaker, resulting in cracks appearing on the surface. By this, the threshold at which cracks appear on the PDMS is the same as that which scission becomes more dominant than cross–linking.

Lichtenberg Figures

Lichtenberg figures are branching patterns which can appear on the surface or interior of insulating materials. Insulators have a minimum required voltage, known as the breakdown voltage, for the material to become electrically conductive. This breakdown voltage is unique to the material and depends on the electrode geometry and gap. Once this minimum is reached, a current creates a weakened path within the material causing permanent molecular and physical changes. This current, referred to as electric discharge, results from the deterioration of the voltage at the surface of the sample within the material [Keim]. The proton irradiation in our experiment causes a high voltage buildup at the surface of the PDMS. Figure 9 leads us to believe that electric discharge is occurring in our samples. The breakdown voltage for PDMS ranges from around 250-635 V/micrometer. After calculating the potential at the surface of our samples using the following

equation

$$V = \int E \cdot dl \tag{4}$$

we find the potential at the the surface around 1.2 MV/micrometer. This potential exceeds the breakdown voltage for our samples, indicating that the Lichtenberg figures seen may be a result of electric discharge. With this magnitude of potential, we would expect to see Lichtenberg figures on all of our irradiated samples. However, we have only seen discharge occur on oxidized samples; although not all oxidized samples show discharge.

Ordered Surface Patterns

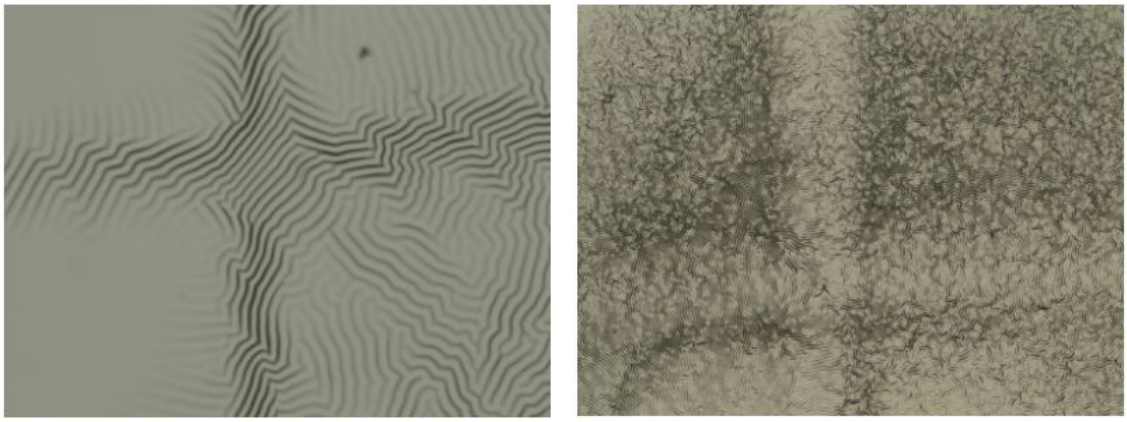

11A 11B

Figure 11: Images take of PDMS samples showing ordered surface patterns. Image A and B were irradiated at a fluence of $1 \times 10^{15}\text{cm}^{-2}$. Image A corresponds to sample E2 and image B corresponds to sample D3 on the chart in the appendix.

We began to see ordered surface patterns on samples irradiated at low fluences ($1 \times 10^{15}\text{cm}^{-2}$ and lower). Some images display a grid–like pattern, resulting from the protons being blocked by the grid located at the entrance into the target chamber. In image 11A, the grid shape is where the surface patterns occur. However, the opposite is true for image 11B; the grid shape is where the ordered surface patterns do not appear as predominantly. Upon further investigation, we found that the sample in image 11A was irradiated for a longer period of time than the sample in image 11B. This could mean that the ordered surface patterns are a time dependent outcome that may only appear within a time window of irradiation.

It is important to note that cracking and the ordered surface patterns are not mutually exclusive. In Figure 12 and we see patterns stretching between cracks. Also, every slide that showed ordered surface patterns shared two properties: they were never oxidized and they never showed any Lichtenberg figures. One possible explanation is that the oxidation process hardens the surface of the PDMS, making it unmalleable. Since the surface is harder, only cracking can occur when the stress becomes too great on the surface of the PDMS. Lichtenberg figures have also only occurred on oxidized slides.

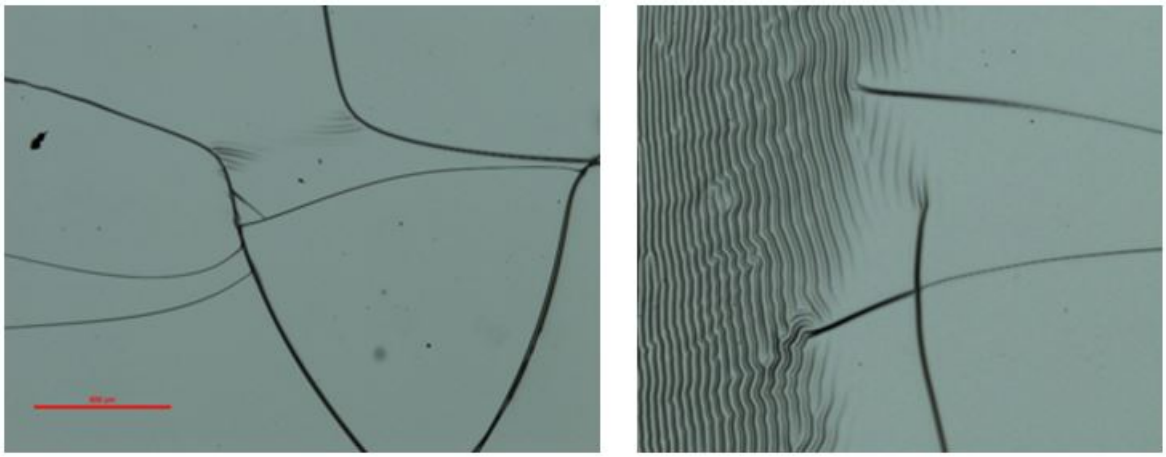

12A 12B

Figure 12: Cracking and surface patterns

MatLab

Using MatLab imaging processes, we can analyze the damage on the PDMS samples. MatLab is a widely used language, which contains a large database of built–in algorithms. Coding in MatLab is effective for both common and domain–specific image formatting, which allows the programmer to both see and change an image [MatLab Manual]. To analyze our data with MatLab, we had to maintain consistency in the lighting, contrast, and magnification of our images. Since the images varied in these categories, we had to even out these characteristics in our images. To do this, we collected the images from the microscope, which we then organized the images by damage types: cracking/Lichtenberg figures and ordered surface patterns. We chose to define damage as any visible morphological defect within our image sample, which is adequate for samples containing cracking and lichtenberg figures. However, this process would give inflated damage

percentages if applied to ordered surface patterns. Thus, we chose to analyze the images with cracking and Lichtenberg figures separate from ordered surface patterns to avoid inconsistencies in our analysis. Ordered surface patterns, due to their unique nature, require a different analysis technique [Puckett].

From there, we looked at each of the images within the same damage type and converted the images into numerical matrices. Each matrix contains numbers that represent the color of the pixel in that location on the image according to MatLabs color map. MatLab interprets each pixel in relation to its RGB values, which consist of three different color matrices: red, green, and blue. To change our images so that we can quantify the damage on the slide, we analyzed our images through just one of these color channels. Arbitrarily, we chose the red channel to use throughout this process. From here the matrix, as read through only the red channel, replaces the initial matrix [Puckett]. This concept is displayed by Figure 13.

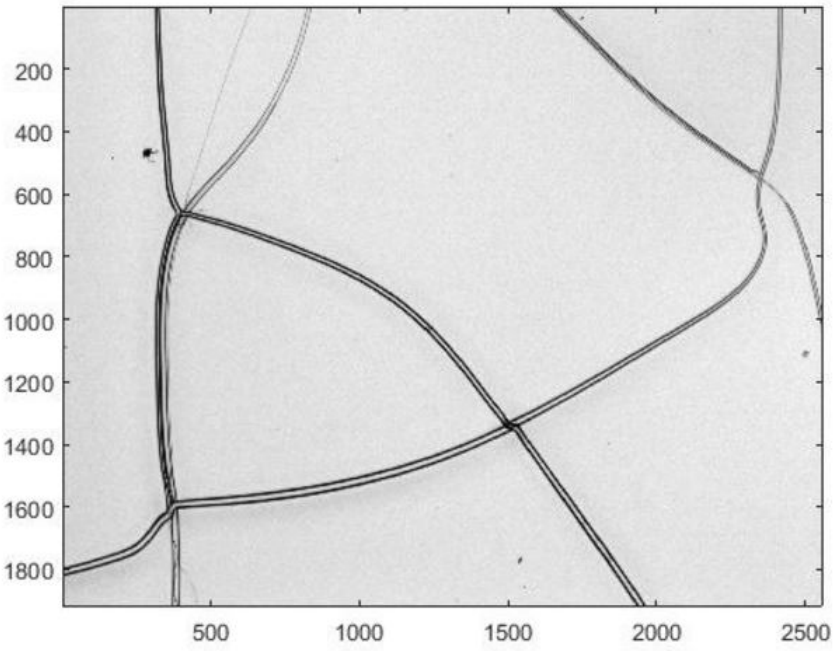

Figure 13: Above is the resulting image of an oxidized PDMS at 2x magnification, under 5×10^{15} cm^{-2} fluence, as analyzed through the initial image's red channel.

We noted that many of the images showed dirt and debris had collected on the slide over the course of our study. MatLab interprets the dirt on the slide images as damage, so in order to maintain accuracy in our quantification of the damage, we had to eliminate evidence of dirt. To

do this, we converted our image matrix into a matrix of doubles and applied a Gaussian filter to it. The Gaussian filter is applied to remove the smaller portions of dirt and dust from the images, as seen in Figure 14.

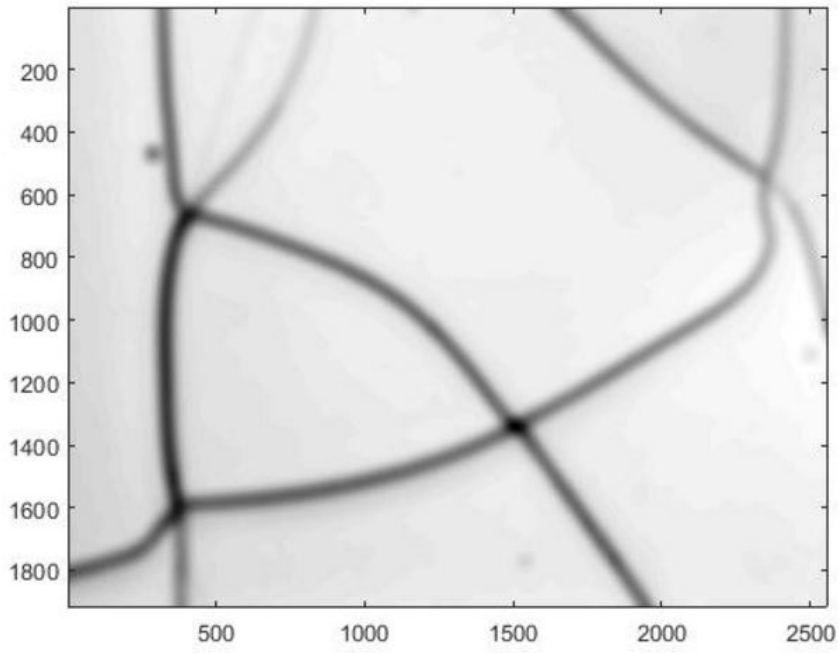

Figure 14: Here, the same image as seen in Figure 13 has a Gaussian filter applied to it, removing small imperfections within the sample.

Once the Gaussian filter has been applied to the image, removing the smaller dirty spots, the newly rendered image matrix was saved. From there, we subtracted the initial image matrix from the Gaussian image matrix. By subtracting these matrices, we created a new matrix in which the dirt and debris was less evident, as shown in Figure 15A. We then took this new matrix and applied a threshold, which set all values below the indicated threshold as zero, resulting in a black and white image. Here, black pixels are associated with a value of zero and white pixels have a value of one [Puckett]. Creating a threshold for the image allowed us to enhance the parts of the image we want to see, while removing everything else. Our code made it possible to set one threshold value as a standard for all images of the same damage type [Puckett] which would remove any inconsistencies with lighting for the original photos taken.

Although the Gaussian filter removes most of the smaller portions of dirt, the bigger pieces

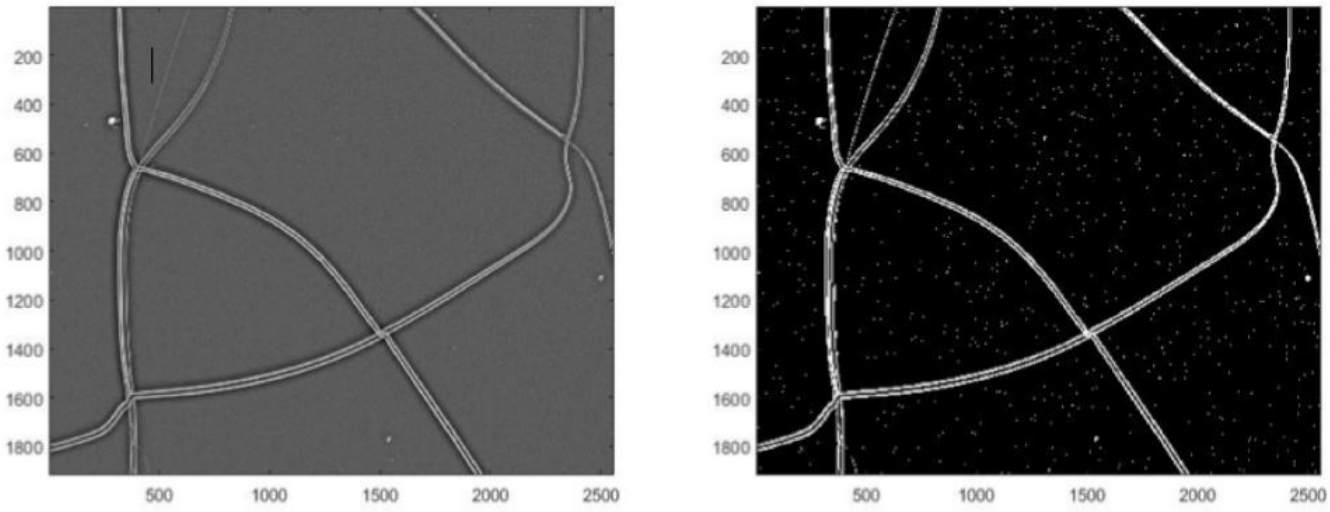

15A 15B

Figure 15: [Left] The figure on the left shows the resulting image created by the subtraction of the original image matrix from the matrix created by the Gaussian. [Right] The figure on the right shows this same image, after thresholding the matrix to read in binary.

of debris still appeared on the image at this time. However, using this black and white matrix, along with a variable called thArea, we were able to completely remove all evidence of dirt from the image.This was done by using a MatLab method known as bwareaopen. This step removes pixels of a connected object if it is smaller than the given object [MatLab Manual].

From here, the matrix is returned as an image containing only the damage we wish to examine for this experiment. For this reason, it was fairly simple to calculate the percent damage of the image by averaging the pixel values, which are all zeroes and ones [Puckett].

The process explained above can be used for images under both cracking/Lichtenberg and ordered surface pattern categories. However, we wanted to take our examination of the ordered surface patterns a step further. Looking from image to image, we saw a clear change in wavelength between each ripple of the ordered surface pattern. We wanted to see if there is a relationship between the wavelength and the fluence used to irradiate the PDMS sample [Puckett].

Our process to analyze the order surface patterns exist as a proof of concept for future work.In order to see if a relationship exists between the fluence and the wavelength, we can zoom in on the images of ordered surface patterns and select a pixel on either side of one ripple. We would select pixels that are approximately centered between the ripples, in order to get a peak-

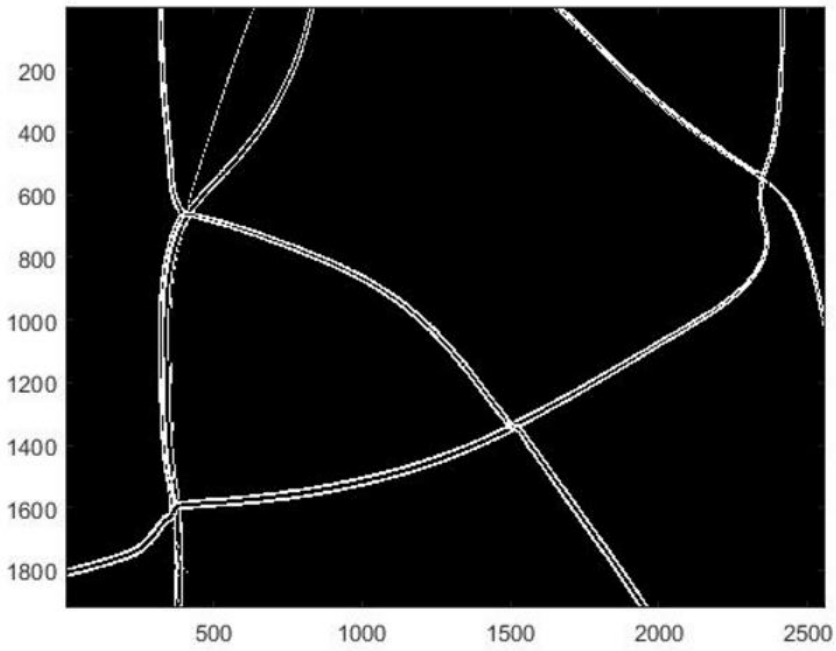

Figure 16: This image exemplifies the final step of our code, which cleans up the bigger areas of dirt and debris using the bwareaopen function [for more information about this function, refer to appendix].

to-peak distance [Puckett]. Peaks are defined as the brightest portions of the ripples. Once we calculate the distance between these pixels, we would repeat this process multiple times for each image. These distances averaged together would allow us to find an average wavelength for the image. This is evident in Figure 16. We could then calculate the standard deviation of the average wavelength. With this information, the wavelength values could be compared to the fluence value of the slide. However, there may be a wide variance in wavelengths across the image. Thus, this method can be updated in future work.

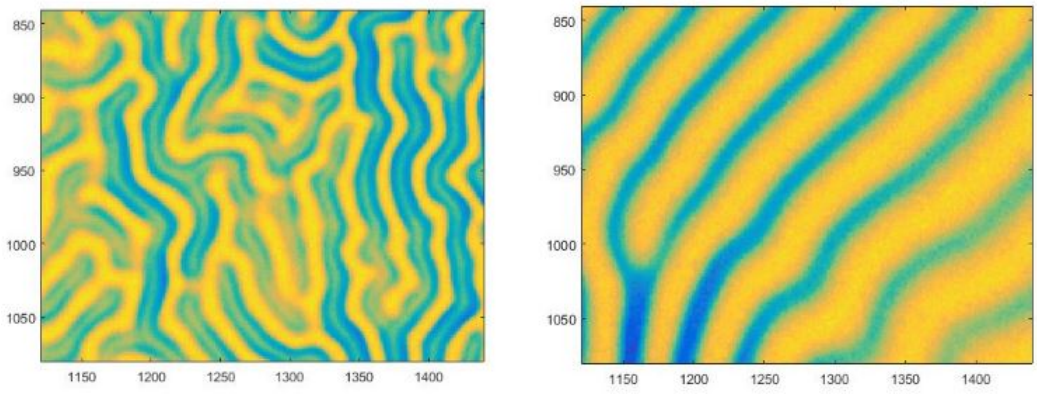

17A 17B

Figure 17: The images above show ordered surface patterns which can be analyzed through the proof of concept explained above.

Quantifying Morphology

The PDMS samples collected were organized by the percent of the slide damaged while corresponding to the fluence the slide experienced. The samples chosen for this graph excluded any samples that contained ordered surface patterns due to our classifications for damage.

The graph above displays the data collected from MatLab analysis in relation to the fluence that the samples experienced. Samples that exhibited ordered surface patterns or had no damage at all were excluded from the graph. Due to the preliminary nature of this graph the error bars in relation to the damage percentage have not been calculated yet. Initially we believed that oxidation would improve the resistivity of the PDMS samples, however the graph above does not support this notion. In order to evaluate the relationship between PDMS and oxidation, a larger sample size could further illustrate this trend.

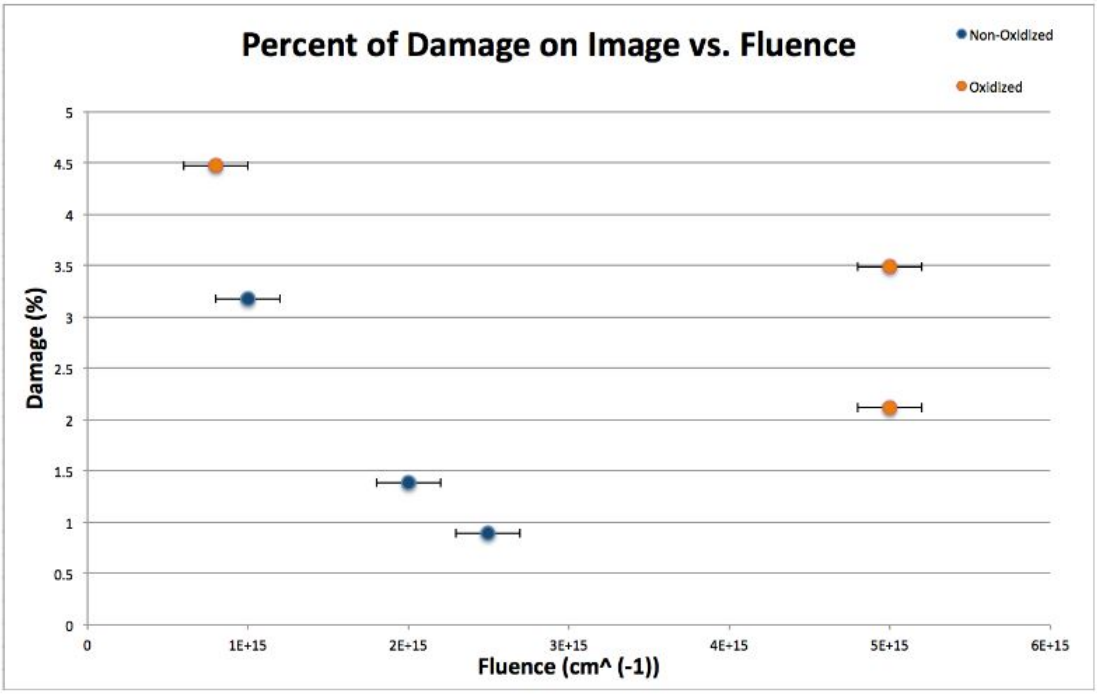

Figure 18: The graph above shows the wide range of damage the slides experienced due to preparation. As shown in this preliminary graph, we do not have enough data to confirm or deny the possibility of a relationship between fluence and the damage percentage.

Conclusion

Our results aligned with those in the works of Xiao, *et al.* and Zhang, *et al.* Despite the discrepancies between these studies, we were able to confirm that proton irradiation causes cracking of silicone. Our results suggest that there is a fluence threshold necessary to cause damage to PDMS under proton irradiation at fluence levels of 8×10^{14} cm^{-2}. Our threshold value is closer to the value found in the works of Xiao, *et al.* than that of Zhang, *et al.* [Xiao][Zhang]. Xiao's research concluded the threshold of silicone to be 5×10^{14} cm^{-2}, while Zhang's was 1×10^{15} cm^{-2} [Zhang].

Another goal of our research was to investigate the effects of oxidation on the surface of PDMS under proton irradiation. During oxidation, PDMS undergoes cross–linking increasing the resistivity which could allow our samples to withstand higher levels of fluence. By examining the amount of fluence oxidized samples are exposed to, this treatment could prove beneficial for PDMS to withstand these low energy protons. If this is the case, then this will improve the longevity of PDMS under these harsh conditions and prove beneficial for future projects similar to the Chandra.

Our data has shown a slight trend in the ability of oxidized samples to withstand higher fluences. However, oxidation does not eliminate damage completely, leaving room for improvement. Many of our oxidized samples showed the Lichtenberg figures, which has not been referenced in previous literature. Future research would help to solidify our understanding of how oxidation affects the irradiation of silicone.

References

[1] AlbrightTech. ”Silicone Rubber.” *Albright Technologies.* N.p., n.d. Web. 13 Sept. 2016.

[2] Allen, Alana. *The Degradation of Silicone Rubber Due to Proton Irradiation.* N.p., Dec. 2015. Print. 27 Sept. 2016.

[3] Berdichevsky, Yevgeny, et al. ”UV/ozone modification of poly (dimethylsiloxane) microfluidic channels.” *Sensors and Actuators B: Chemical* 97.2 (2004): 402-408.

[4] Booz, Michael, Zack Jaouni, Kyle Labowski, and Will Vanderpoel. *Degradation of PDMS via Irradiation.* N.p., 19 Dec. 2015. Print.

[5] Borjanovic V., L. Bistricic, I. Vlasov, K. Furic, I Zamboni, M. Jaksic, O. Shenderova, ”Influence of Proton Irradiation on the Structure and Stability of Poly(dimethylsiloxane) and Poly(dimethylsiloxane)-nanodiamond Composite.” J. Vac. Sci. *Technol. B Journal of Vacuum Science & Technology B: Microelectronics and Nanometer Structures* 27.6 (2009)

[6] Di, Mingwei, et al. ”Radiation effect of 150keV protons on methyl silicone rubber reinforced with MQ silicone resin.” *Nuclear Instruments and Methods in Physics Research Section B: Beam Interactions with Materials and Atoms* 248.1 (2006): 31–36.

[7] Ebewele, Robert Oboigbaotor. Polymer Science and Technology. Boca Raton: CRC, 2000. Print.

[8] Gonzlez-Prez, Giovanni, and Guillermina Burillo. *”Modification of Silicone Sealant to Improve Gamma Radiation Resistance, by Addition of Protective Agents.” Radiation Physics and Chemistry* 90 (2013): 98-103. Web.

[9] Grun, Alex, Private Communication, Nov 19 2016.

[10] Industry, Essential Chemisty. ”CIEC Promoting Science at the University of York, York, UK.” *Silicones*. CEIC Promoting Science, 18 Mar. 2013. Web. 30 Nov. 2016.

[11] Keim, Robert. *Physics Of Conductors And Insulators - Electronics Textbook*. EETech Media, n.d. Web. 30 Nov. 2016.

[12] Kuphaldt, Tony R. ”Insulator Breakdown Voltage.” *Insulator Breakdown Voltage : Physics Of Conductors And Insulators*. All About Circuits, 18 Oct. 2006. Web. 26 Sept. 2016.

[13] LaBel, Kenneth. ”Single Event Effects.” NASA. (2015)

[14] Leonov, Arkadii. ”Damage of Cross–Linked Rubbers as the Scission of Polymer Chains: Modeling and Tensile Experiments.” (2012): 2049–2065.

[15] M. C. Weisskopf, B. Brinkman, C. Canizares, G. Garmire, S. Murray, and L. P. Van Speybroeck (January 2002), An Overview of the Performance and Scientific Results from the Chandra XRay Observatory. Publications of the Astronomical Society of the Pacific, Vol. 114, No. 791 pp. 1-24.

[16] MatLab Manual, "Documentation." *MATLAB Documentation*. N.p., n.d. Web. 15 Dec. 2016. <https://www.mathworks.com/help/matlab/>.

[17] Murray, M.J (2010)., Energy Calibrations, Thin Targets, and Rutherford Scattering Experiments with the Gettysburg College Proton Accelerator

[18] Olah, Attila, Henrik Hillborg, and G. Julius Vancso. "Hydrophobic recovery of UV/ozone treated poly (dimethylsiloxane): adhesion studies by contact mechanics and mechanism of surface modification." *Applied Surface Science* 239.3 (2005): 410-423.

[19] Ouyang M., C. Yuan, R. J. Muisener, A. Boulares, J. T. Koberstein, Conversion of Some Siloxane Polymers to Silicon Oxide by UV/Ozone Photochemical Processes, *Chem. Matter* 12, pp. 1591 1596 (2000)

[20]Prigozhin, G., Kissel, S., Bautz, M., Grant, C., LaMarr, B., Foster, R., Ricker, G. (2000) Characterization of the radiation damage in the Chandra X-ray CCDs .Proc. SPIE Vol.4140 pp.123-134

[21] Puckett, James, Private Communication, Nov 19 2016. [22] Rossiter C., B. Crawford, and S. Stephenson, Qualitative Damage to Organic Silicone due to 200keV Proton Irradiation, Gettysburg College, Gettysburg, PA (2013)

[23] Sarmoria C., Model for a Scission-Crosslinking] C. Sarmoria, V. Enrique, "Model for a Scission-crosslinking Process with Both H and Y Crosslinks." *Polymer* 45.16, pp. 5661-5669 (2004)

[24] Stephenson, Sharon, Private Communication, Nov 21 2016.

[25] Vig, John R. "UV/ozone cleaning of surfaces." *Journal of Vacuum Science* & Technology A 3.3 (1985): 1027-1034.

[26]] Xiao, Haiying, et al. "Optical degradation of polydimethylsiloxane under 150 keV proton exposure." *Journal of applied polymer science* 109.6 (2008): 4060–4064.

[27] Zhang, Lixin, et al. "Effect of 200keV proton irradiation on the properties of methyl silicone rubber." *Radiation Physics and Chemistry* 75.2 (2006): 350–355.

Appendix 1

Creation of Chlorosilanes:

Silicon metal mixed with Chloromethane to create silanes [Industry]

Chlorosilane formation:

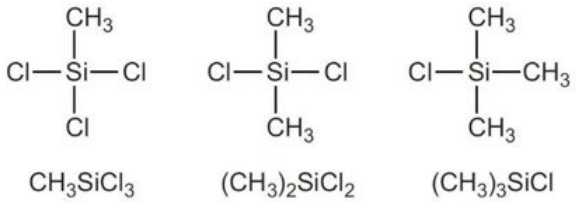

Different possible chlorosilanes formations, $(CH_3)_2$ Si Cl_2 is most common to be formed in this reaction. [Industry]

Hydrolysis:

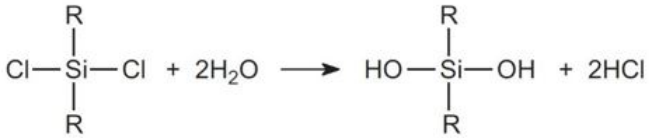

R is representative of organic compound, CH_3 in the case of PDMS. The chlorosilanes mixed with water creates the disilanol. [Industry]

Condensation Polymerization:

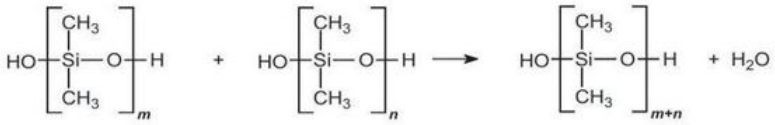

Acidic catalyst with disilanol causes the Si-O section to connect and repeat over and over, forming the long chains of silicone. [Industry]

Appendix 2

Final Crack and Lichtenberg Figures produced by MatLab code:

Each of the following images show PDMS samples, imaged at 2x magnification.

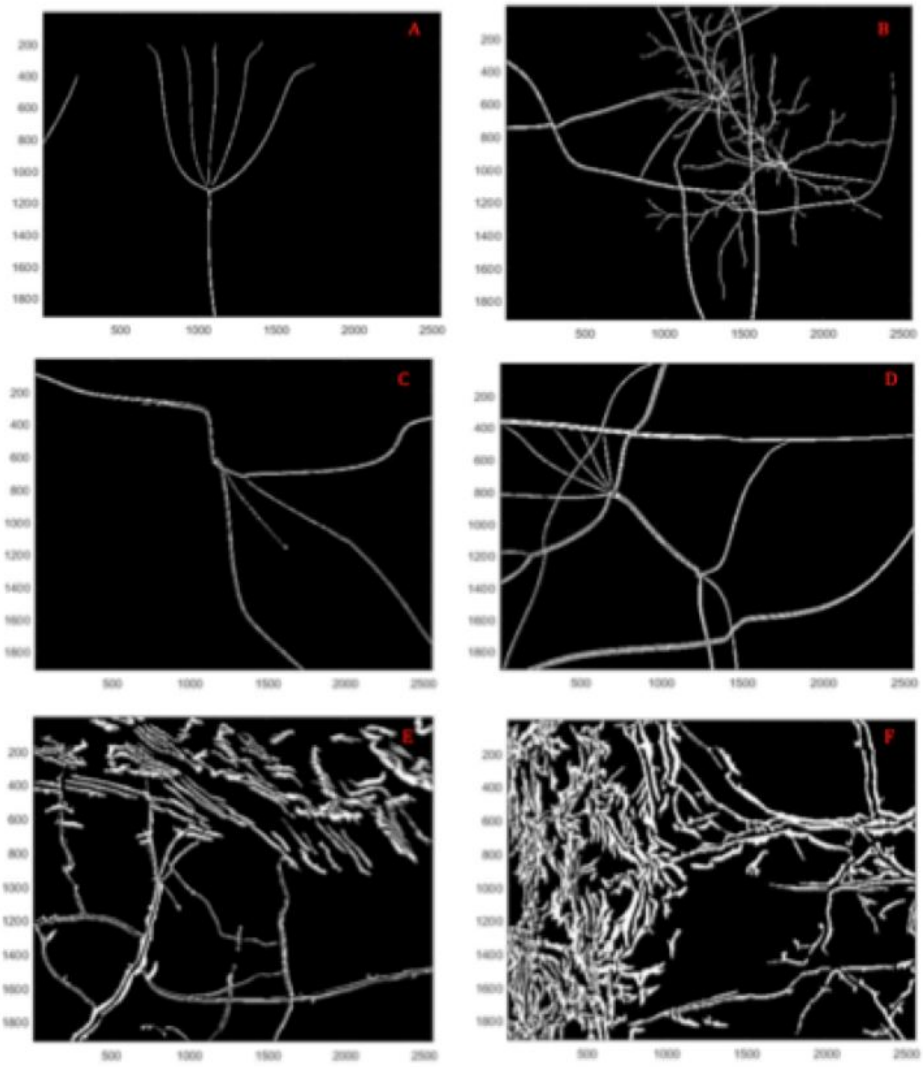

A. Irradiated with 5 x 10^15 cm ^(-1) fluence.
B. Irradiated with 8 x 10^14 cm ^(-1) fluence.
C. Irradiated with 10^15 cm ^(-1) fluence.
D. Irradiated with unknown fluence.
E&F. Irradiated with 2 x 10^16 cm ^(-1) fluence. Sample was not completely dry before irradiated.

Appendix 3

Image Name	Zoom of Image	Counts	Fluence	Oxidized (Y/N)	Discolored (Y/N)	Discharge (Y/N)	Pattern (Y/N)	Threshold	Percent Damaged
C1	2x	3102375	5 x 10^15	Yes	No	Yes	No	0.025	0.0211
C3	2x	655476	1 x 10^15	No	No	Yes	No	0.025	0.0318
D1	2x	102375	5 x 10^15	Yes	No	No	No	0.025	0.0349
D2	2x	590901	8 x 10^14	Yes	No	Yes	No	0.025	0.0447
F2	2x	Unknown	2 x 10^15	No	No	No	No	0.025	0.0138
F3.2	2x	2500000	2.5 x 10^15	No	No	Yes	No	0.025	0.0089

Table 1. The above table shows the slides that experienced cracking or Lichtenberg figures. These images analyzed using MatLab. The highlighted samples noted that the sample was oxidized.

Image Name	Zoom of Image	Counts	Fluence	Oxidized (Y/N)	Discolored (Y/N)	Discharge (Y/N)	Pattern (Y/N)
A1	2x	520000	10^15	No	No	No	Yes
D3	2x	655476	10^15	No	No	No	Yes
E2	2x	570000	10^15	No	No	No	Yes (in second image)
E3	2x	57000	10^14	No	No	No	Yes
F1	2x	310000	8x 10^14	No	No	No	Yes

Table 2. The above table shows the slides that displayed ordered surface patterns.

Image Name	Zoom of Image	Counts	Fluence	Oxidized (Y/N)	Discolored (Y/N)	Discharge (Y/N)	Pattern (Y/N)	Threshold	Percent Damaged
A2	2x	660000	10^15	No	No	No	Yes		
A3	2x	550000	10^15	Yes	No	Yes	No	Too	Dirty
B1	2x	78000	10^15	Yes	No	No	No		
B2	2x	85864	10^14	Yes	No	No	No	To	Use
B3	2x	84547	10^14	No	No	No	No		
C2	2x	590961	8 x 10^14	Yes	No	No	No	Too	Dirty
E1	2x	3120000	2 x 10^16	Yes	Yes	No	Different kind	Not	Visible
F3.1	2x	2500000	2.5 x 10^15	No	No	Yes	No		

Table 3. The above table shows slides that we were unable to use for analysis.

Appendix 4

B (G)	Channel	Energy (KeV)	Corrected E (keV)	Geometrical E (keV)	Difference	% Difference
678.8	163	54.2	60.6	53	7.5	14
788.7	227	74.2	80.6	71.6	9	13
881.4	290	94	100	89.4	10.6	12
952.5	344	111	116.7	104.4	12.2	12
1058.6	432	138.7	143.8	129	14.8	11
1059	436	139.9	145	129.1	16	12
1147	506	161.9	166.8	151.4	15.4	10
1146.3	507	162.2	167.2	151.2	15.9	11
1220	582	185.8	190.4	171.3	19.1	11
1280.4	641	204.3	208.8	188.7	20.1	11
1318.3	679	216.2	220.6	200	20.6	10